Sensing and Bio-Sensing Research 29 (2020) 100366

Contents lists available at ScienceDirect

Sensing and Bio-Sensing Research

journal homepage: www.elsevier.com/locate/sbsr

The first attempt on fabrication of a nano-biosensing platform and exploiting first-order advantage from impedimetric data: Application to simultaneous biosensing of doxorubicin, daunorubicin and idarubicin

Shokoufeh Soleimani[a], Elham Arkan[b], Tooraj Farshadnia[a], Zahra Mahnam[a], Faramarz Jalili[a], Hector C. Goicoechea[c], Ali R. Jalalvand[a,*]

[a] Research Center of Oils and Fats, Research Institute for Health Technology, Kermanshah University of Medical Sciences, Kermanshah, Iran
[b] Nano Drug Delivery Research Center, Research Institute for Health Technology, Kermanshah University of Medical Sciences, Kermanshah, Iran
[c] Laboratorio de Desarrollo Analítico y Quimiometría (LADAQ), Catedra de Química Analítica I, Universidad Nacional del Litoral, Ciudad Universitaria, CC242 (S3000ZAA), Santa Fe, Argentina

ARTICLE INFO

Keywords:
Doxorubicin
Daunorubicin
Idarubicin
Simultaneous determination
Multivariate calibration
Impedimetry

ABSTRACT

In this work, for the first time, we have developed a novel and very interesting electroanalytical methodology assisted by first-order multivariate calibration (MVC) for simultaneous determination of doxorubicin (DX), daunorubicin (DN) and idarubicin (ID) as three chemotherapeutic drugs at simulated physiological conditions. A sever overlapping was observed among signals of the three drugs which hindered us for simultaneous determination of them by conventional electroanalytical techniques. Therefore, we had to assist our method by chemometric approaches to develop a novel method for simultaneous determination of DX, DN and ID. Among the existing electroanalytical methods, electrochemical impedance spectroscopy (EIS) due to its high sensitivity was chosen. After individual calibration of the three drugs with the EIS data, a set of calibration samples was designed which was used to develop several first-order MVC models by partial least squares (PLS), continuum power regression (CPR), radial basis function-partial least squares (RBF-PLS), RBF-artificial neural network (RBF-ANN) and least squares-support vector machines (LS-SVM) as linear and non-linear chemometric algorithms. Then, performance of the developed MVC models in predicting concentrations of DX, DN and ID in synthetic samples was compared to choose the best model for the analysis of real samples. Our records confirmed more superiority of RBF-PLS algorithm than the other developed models which motivated us to choose it for the analysis of real samples. Fortunately, the results of the RBF-PLS in the analysis of real samples towards simultaneous determination DX, DN and ID was acceptable.

1. Introduction

Cancer is one of the most serious human diseases in the world and it is divided into many main sub-cancers dependent on the involved tissue. Leukemia or blood cancer is one of the most common types of cancer around the world [1]. Leukemia is divided into acute and chronic types depending on the range, severity, and progression rate of the disease. In acute leukemia, rapid growth is followed by the production of several immature white blood cells, and the interval between the incidence of disease and its progression is very short. In chronic leukemia, slow growth is accompanied by the production of a greater number of mature cancer cells, and the interval between the incidence of disease and its progression is longer [2,3]. A predisposing and prominent factor involved in the presentation of leukemia, like any other cancer, is disrupted cell division. Previous history of some blood disorders or cancer, genetic factors, host susceptibility, radiation, tobacco addiction, environmental pollutants, impaired immune system, and age increase cause acute leukemia. For the treatment of acute leukemia, chemotherapy, radiotherapy, bone marrow transplantation, and stem cells are used. The chemical drugs used for chemotherapy affect the cell division of cancer cells. Among the existing drugs, doxorubicin (DX), daunorubicin (DN), and idarubicin (ID) have a special place in the treatment of leukemia [4–6]. The exact mechanism of the DX, DN, and ID is binding to DNA and inhibiting nucleic acid production by destroying the molecular structure and making a space barrier. However, they make many side effects such as anemia, hair loss, nausea, vomiting, diarrhea, allergic reaction, ringing in ears and hearing loss, fertility impairment, mouth ulcers, bronchospasm, fever and flu-like

* Corresponding author.
E-mail address: ali.jalalvand1984@gmail.com (A.R. Jalalvand).

https://doi.org/10.1016/j.sbsr.2020.100366
Received 27 May 2020; Received in revised form 1 July 2020

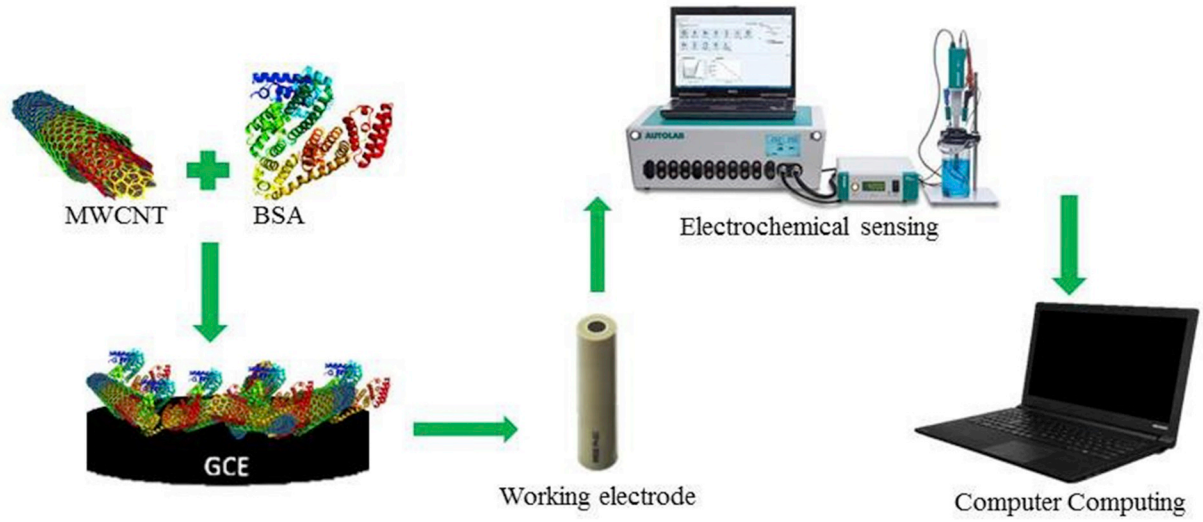

Scheme 1. Schematic representation of the steps of the study presented in this work.

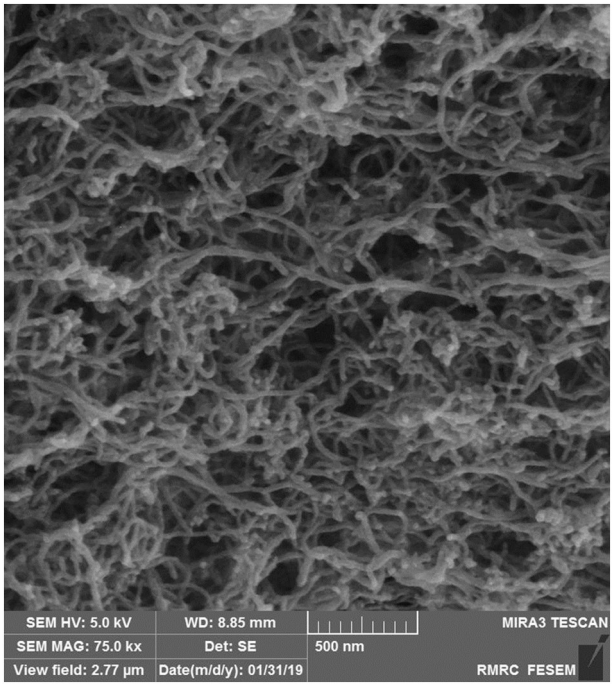

Fig. 1. The SEM image captured from the surface of MWCNTs-BSA/GCE.

symptoms, and secondary malignancies [7,8]. Therefore, determination of DX, DN and ID are very important from clinical point of view.

There are some analytical techniques such as UV–Vis spectrophotometry, FT-IR [9], electrochemistry [10], high performance liquid chromatography (HPLC) [11], capillary electrophoresis [12], and nuclear magnetic resonance (NMR) [13] which can be used to determine drugs in blood. Although these methods are accurate and reliable but, they are expensive and time-consuming which motivated researchers to develop new methods. Electrochemists due to having simple, fast, sensitive, inexpensive, selective, reproducible and repeatable methods can develop new techniques to tackle the mentioned problems. It is important to be mentioned achieving the lowest detection limit is one of the most important limitations of these methods [14,15,16]. Therefore, electrochemical methods could be assisted by nanomaterials or nanostructures which can help electrochemists to increase the surface area, binding sites and response signal of their electrodes. Moreover, the selectivity of the electrochemical methods can be increased by the use of chemometric techniques [17]. First-order multivariate calibration (MVC) which operates using a vector of data per sample can predict concentrations of the analytes of interest in an interfering medium provided they are included in the calibration set, a property known as the “first-order advantage”. Complex processes, perturbation of the excitation signal, large field currents, large amount of information produced by electrochemical devices, large overlap with the signal of other analytes and possible disturbances within the sample tissue indicate the necessity of using chemometrics along with electrochemical methods [17–21]. Among the existing electrochemical methods, electrochemical impedance spectroscopy (EIS) is a simple and sensitive technique which has been frequently used for quantitative purposes [22,23]. But, in this work, we are going to use the EIS for simultaneous determination of DX, DN and ID which is reported for the first time. Voltammetric signals of DX, DN and ID showed a severe overlapping which hindered us to determine them simultaneously by conventional methods. Another problem arising from voltammetric signals was related to their sensitivity which forced us to use EIS which was more sensitive than voltammetric techniques. Although the EIS method is sensitive but is not able to tackle the overlapping problem, but the EIS technique can be assisted by chemometric methods to overcome this challenge. Coupling of the EIS method with chemometric method will produce a very interesting method which could be used for quantitative purposes.

In this work, we are going to develop a novel chemometrics assisted-electroanalytical methodology for simultaneous biosensing of DX, DN and ID based on generation of first-order EIS data and using them for building MVC models with the help of partial least squares (PLS), continuum power regression (CPR), radial basis function-partial least squares (RBF-PLS), RBF-artificial neural network (RBF-ANN) and least squares-support vector machines (LS-SVM) as first-order multivariate algorithms. To increase the sensitivity and selectivity of the developed methodology, the bare glassy carbon electrode (GCE) will be modified by a composite film consisting of multiwall carbon nanotube (MWCNTs) and bovine serum albumin (BSA). After checking the performance of the developed MVCs for prediction of concentration of DX, DN and ID in synthetic samples, the best model will be applied to the analysis of serum samples as real cases. A schematic representation of the steps of the developed methodology in this work is shown in Scheme 1.

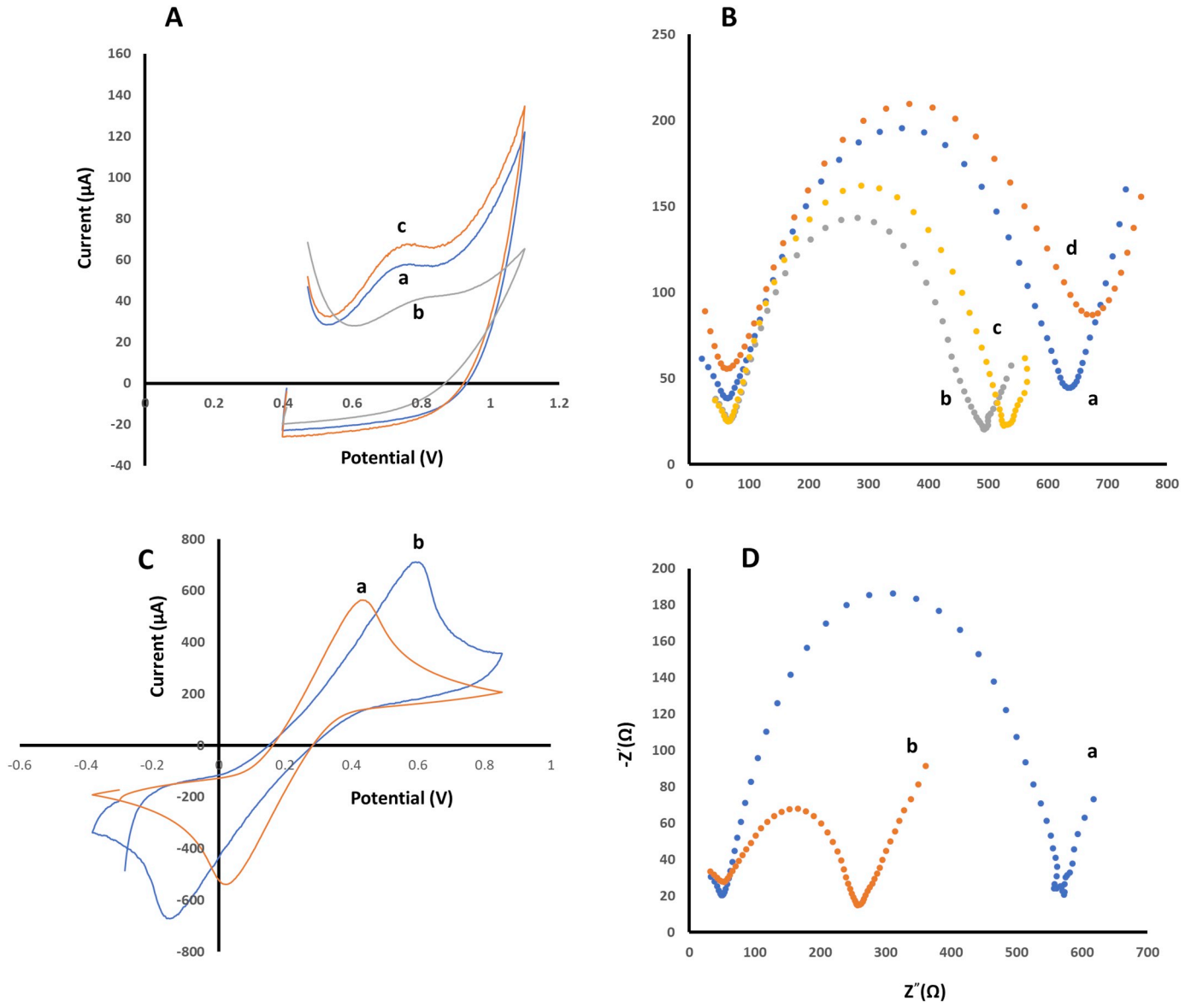

Fig. 2. (A) CVs of (a) DX (50 μM), (b) DN (50 μM) and (c) ID (50 μM) recorded in PBS (0.1 M, pH 7.4) at the surface of MWCNTs-BSA/GCE at the scan rate of 50 mV s^{-1}, (B) EISs of 50 μM (a) DX, (b) DN, (c) ID and (d) their mixture recorded in 0.05 M electrochemical probe at the surface of MWCNTs-BSA/GCE, (C) CVs of (a) GCE and (b) MWCNTs-BSA/GCE in 0.05 M electrochemical probe, scan rate 0.05 mVs^{-1}, and (D) EISs of (a) GCE and (b) MWCNTs-BSA/GCE in 0.05 M electrochemical probe.

2. Experimental

2.1. Chemicals and solutions

The DX, DN, ID, MWCNTs, ethanol (EtOH), dimethylformamide (DMF), BSA, KCl, NaH_2PO_4, Na_2HPO_4, H_3PO_4, NaOH, $K_3[Fe(CN)_6]^{3-}$ and $K_4[Fe(CN)_6]^{4-}$ were purchased from Sigma-Aldrich. A phosphate buffered solution (PBS, 0.1 M, pH 7.4) was prepared from NaH_2PO_4 and Na_2HPO_4. Stock standard solutions of DX, DN and ID (0.01 M) were prepared by dissolving their solid powder in the PBS. A probe solution with a concentration of 0.05 M was prepared by dissolution of $K_3[Fe(CN)_6]^{3-}$ and $K_4[Fe(CN)_6]^{4-}$ in KCl. 10 mg MWCNTs was added to 1 mL DMF and ultrasonicated for 1 h to obtain a homogeneous gel-like solution. An optimized amount of BSA (0.1 mg) was dissolved in a mixture of EtOH/PBS (20/80, *V*/V) and then, 200 μL of this mixture was added to 800 μL of the prepared gel-like solution of MWCNTs to prepare MWCNTs-BSA. All the solutions were prepared by doubly distilled water (DDW).

2.2. Apparatus and software

An Autolab (302N) controlled by the NOVA software (Version 1.8) was used for recording electrochemical data. A bare or modified GCE, a Pt wire and an Ag/AgCl electrode were used as working, counter and reference electrode, respectively. By using a JENWAY-3510 pH meter, pH of the solutions was adjusted. All the chemometric algorithms were run in MATALAB (Version 7.5) environment. Scanning electron microscopic (SEM) images were taken by using a MIRA3TESCAN-XMU. A DELL XPS laptop (L502X) with 8 GB of RAM, Intel Core i7-2630QM 2.0 GHz and Windows 10 as its operating system was used for running all calculations.

2.3. Preparation of the sensor

The bare GCE was polished on a silky pad impregnated with alumina slurry and then, rinsed with DDW and dried at room temperature. Modification of the bare GCE was performed by drop-casting of 10 μL

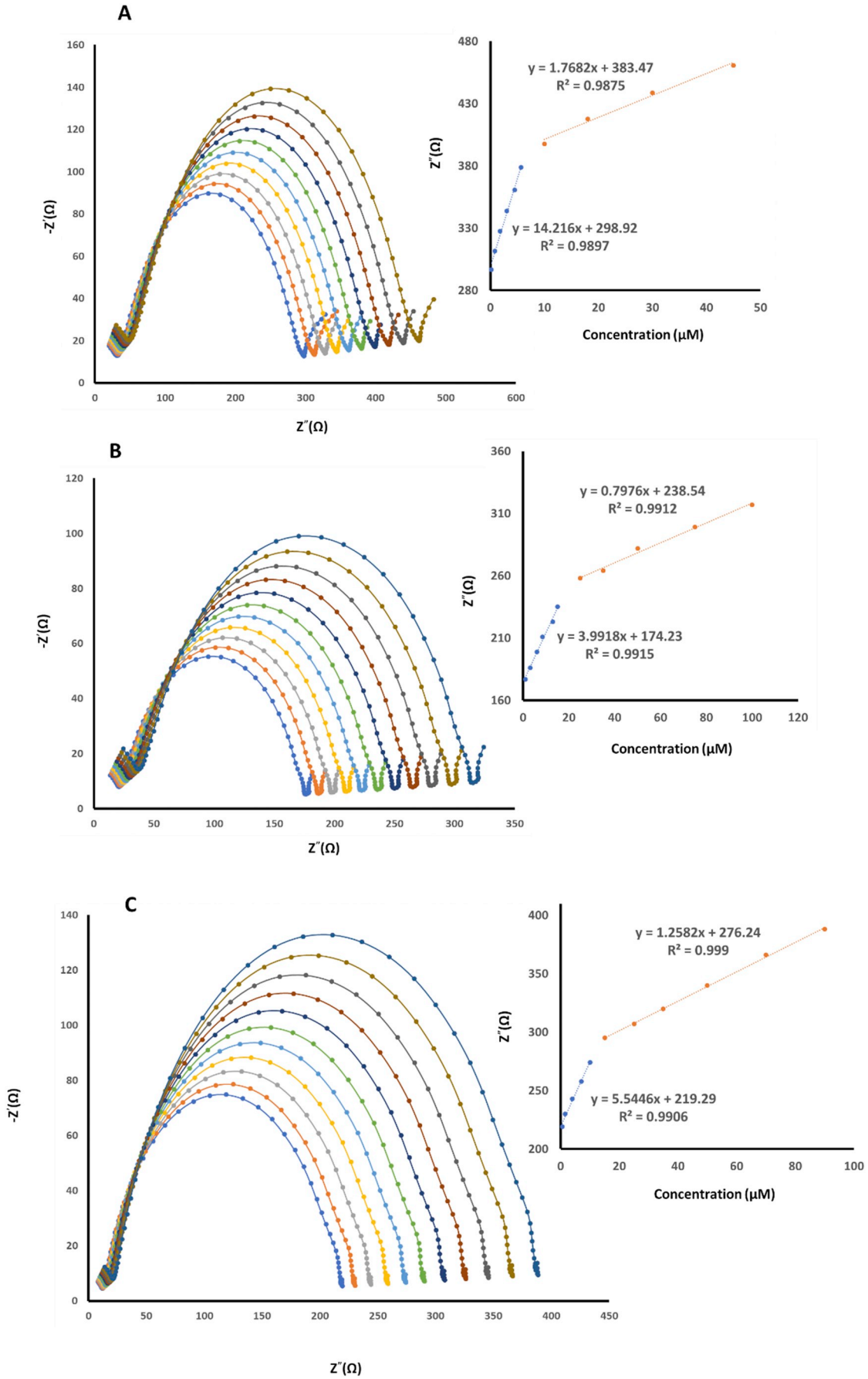

Fig. 3. EIS responses of MWCNTs-BSA/GCE to (A) DX, (B) DN and (C) ID. Insets show calibration graphs.

Table 1
Compositions (μM) of the mixtures related to the calibration and validation sets.

Calibration set				Validation set			
Sample No.	DX	DN	ID	Sample No.	DX	DN	ID
1	0.2	1	0.5	1	5	20	5
2	0.2	1	90	2	10	25	10
3	0.2	100	0.5	3	12	12	2.5
4	0.2	100	90	4	30	45	14
5	33	1	0.5	5	20	50	18
6	33	1	90	6	7	6	25
7	33	100	0.5	7	4	10	30
8	33	100	90	8	15	14	65
9	0.2	50	45	9	40	11	80
10	45	50	45	10	45	13	70
11	22.5	1	45				
12	22.5	1	45				
13	22.5	50	0.5				
14	22.5	50	0.5				
15	22.5	50	45				

Table 2
Predicted concentrations (μM) of the validation set by different algorithms.

	PLS			CPR		
Sample NO.	DX	DN	ID	DX	DN	ID
1	3.8	18.3	5.7	6	18.7	4.5
2	8.5	23	11.7	11.3	23.4	11.2
3	13.5	13.5	2.15	13.2	11	2.32
4	32.5	42	15.6	32	42.5	15.1
5	17.5	52.7	19.2	22.5	48	17
6	8.7	7.8	22.6	5.5	7	27
7	5	8.1	28.1	4.8	8.5	28.5
8	13.7	17	62.5	14	11.5	63.2
9	43	12.9	77.2	37.5	12.3	78
10	48.3	15	73.4	48	14.6	68.1
	RBF-PLS			RBF-ANN		
Sample NO.	DX	DN	ID	DX	DN	ID
1	5.1	20.2	5.03	5.5	20.5	5.1
2	9.9	24.8	9.9	10.6	24.5	10.3
3	11.85	11.9	2.45	12.5	11.7	2.6
4	30.2	46	13.95	31	46.3	14.1
5	20.15	50.5	18.1	21.5	49	17.7
6	6.85	5.9	25.3	6.3	5.7	26.2
7	4.05	10.2	30.3	4.1	10.4	30.6
8	15.2	14.3	65.5	14.4	14.7	66
9	39.5	10.6	80.1	42	11.8	81
10	46	13.3	70.2	43	13.6	71
LS-SVM						
Sample NO.	DX		DN		ID	
1	5.9		21		5.35	
2	11		26.2		10.8	
3	11		11.5		2.7	
4	28.5		47		14.5	
5	18		51.5		18.6	
6	6		6.6		26.5	
7	4.4		11		31	
8	15.7		15.2		63.7	
9	38		12		81.5	
10	42.5		12		71.6	

MWCNTs-BSA onto its surface. After drying the MWCNTs-BSA/GCE at room temperature, it was covered and kept in a refrigerator. The SEM image taken from the surface of MWCNTs-BSA/GCE is shown in Fig. 1. As can be seen, the tubes of the MWCNTs in combination with BSA have been twined around each other and covered the whole of electrode surface which confirmed the successfulness of the fabrication process.

2.4. Preparation of the real samples

Three blank human serum samples (drug free) were prepared according to the procedure described by Shu et al. with some modifications [24]. Elimination of the protein and other substances was performed by pouring 5.0 mL of each serum sample in a 10.0 mL glass tube containing 5.0 mL zinc sulfate solution-acetonitrile 15.0% (*w/v*) and the tube was vortexed for 20.0 min followed by centrifugation at 4000 rpm for 5 min. Then, the supernatant was collected in the same tube and the solution was used for the next analyses.

3. Results and discussion

3.1. Electrochemical studies

All the electrochemical data reported in this work were recorded in the PBS (0.1 M, pH 7.4) at room temperature. The first attempt for starting the work was focused on recording cyclic voltammetric (CV) responses of the MWCNTs-BSA/GCE to DX, DN and ID and the results are shown in Fig. 2A. As can be seen, there was a sever overlapping among the signals of DX, DN and ID which hindered us to determine them by the use of conventional voltammetric techniques. Another, difficulty was related to the low sensitivity of the voltammetric

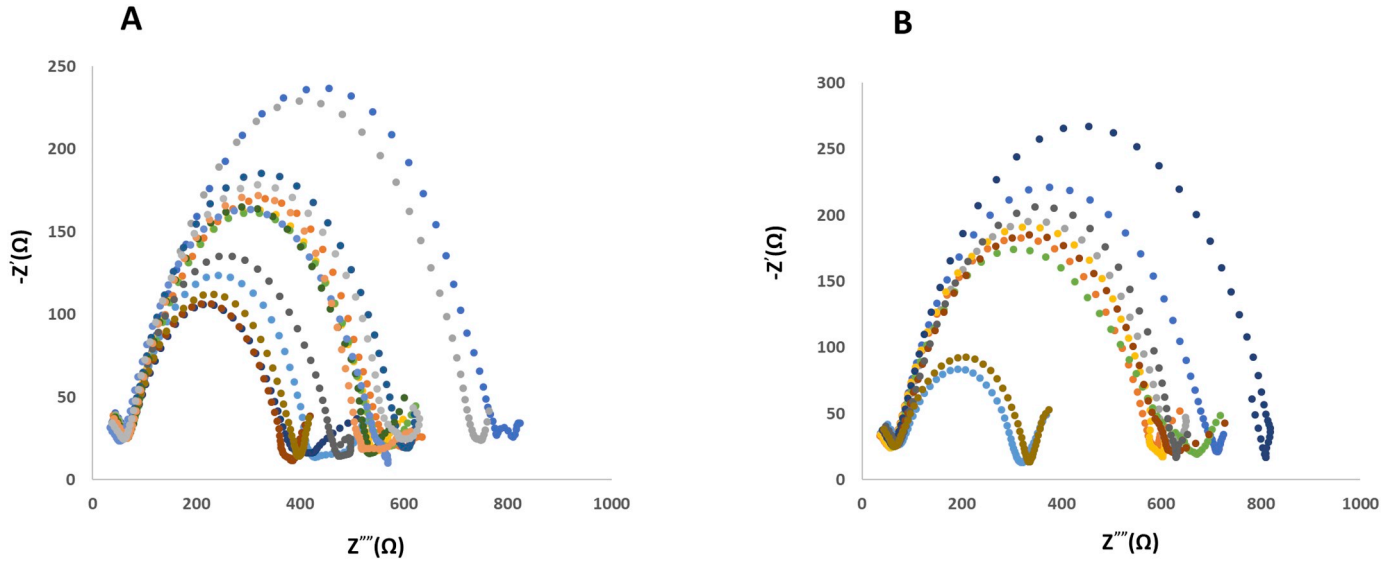

Fig. 4. EIS responses of MWCNTs-BSA/GCE to the mixtures of (A) calibration set and (B) validation set.

Table 3
RMSEP and REP values related to the prediction of validation set.

	PLS			CPR		
	DX	DN	ID	DX	DN	ID
RMSEP	2.09	2.21	2.06	1.83	1.71	1.45
REP	11.15	10.73	6.45	9.74	8.30	4.54
	RBF-PLS			RBF-ANN		
	DX	DN	ID	DX	DN	ID
RMSEP	0.34	0.41	0.22	1.14	0.71	0.71
REP	2	2.02	0.70	6.05	3.43	2.21
	LS-SVM					
	DX			DN	ID	
RMSEP	1.45			1.17	1.06	
REP	7.7			5.69	3.31	

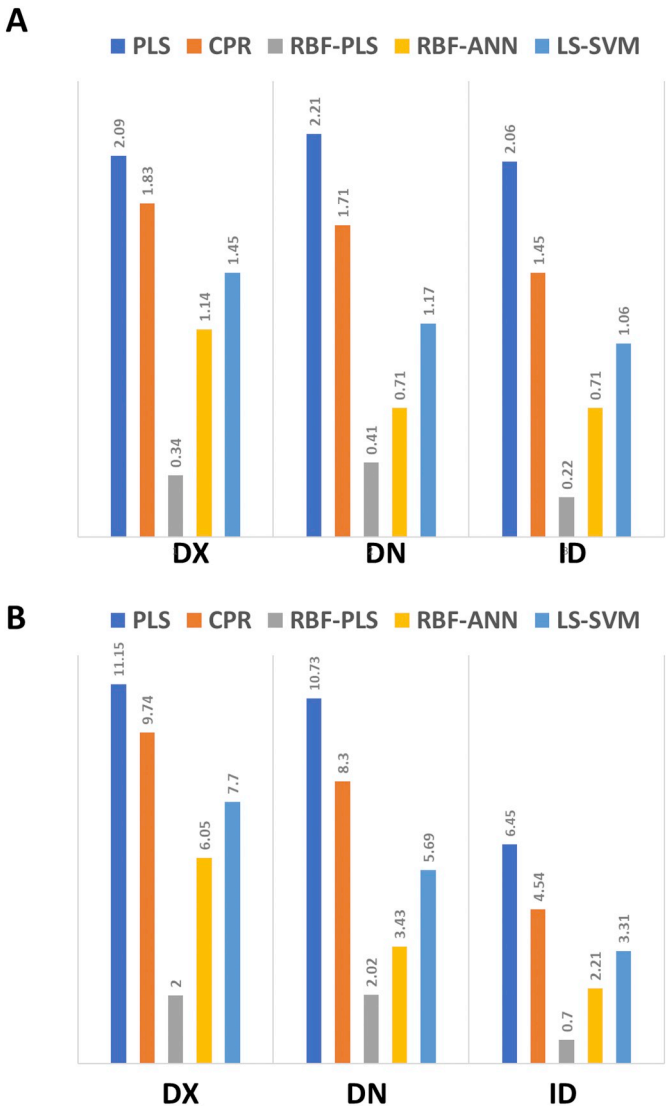

Fig. 5. Graphical comparison of the performance of different first-order algorithms in predicting concentrations of DX, DN and ID based on (A) RMSEP and (B) REP values.

techniques. The mentioned problems motivated us to open new windows for doing the project in a better way. Our strategy to tackle the mentioned problems was including the following steps: 1) using EIS as the operating technique due to its more sensitivity than voltammetric methods, 2) modification of the bare GCE with MWCNTs-BSA/GCE could help to increase the sensitivity of the method due to the presence of MWCNTs and BSA could act as a trap for taking DX, DN and ID molecules and 3) using chemometric techniques to shoot the overlapping trouble. As can be seen in Fig. 2B, the EIS response of the MWCNTs-BSA/GCE to the mixture of DX, DN and ID is a single semicircle which cannot help us to determine them simultaneously. Therefore, the EIS method must be assisted by chemometric method for simultaneous determination of DX, DN and ID. Figs. 2C and D show the CV and EIS responses of GCE (curve *a*) and MWCNTs-BSA/GCE (curve *b*) in electrochemical probe. As can be seen, due to the presence of MWCNTs in the modification process, the MWCNTs-BSA/GCE had a stronger CV and its EIS response had a smaller radius. Although, the presence of BSA caused some trouble in the sensitivity of the developed method but, BSA can help us to increase the selectivity of the developed method. Our methodology will be expanded in more details in next sections.

3.2. Chemometric studies

3.2.1. Why MVC is necessary?

As can be clearly seen from Fig. 2A, CVs of DX, DN and ID are severely overlapped which cannot be simultaneously determined by the use of conventional electrochemical methods. Another problem related the using of conventional voltammetric techniques is related to their sensitivity. To tackle the mentioned problems, we have used the EIS method in combination with chemometric techniques which will be expanded with more details in next sections.

As an important thing, it should be stated that the EIS data are unique data which are changed in both of *X* and *Y* directions when concentration of the analyte is changed. Therefore, for multivariate calibration purposes, the average of *X*-axis and *Y*-axis was used as the input signal.

3.2.2. Calibrations

3.2.2.1. Univariate calibrations. In order to obtain linear ranges of the response of the MWCNTs-BSA/GCE to DX, DN and ID, three individual calibration curves were constructed by recording EIS responses of the sensor to DX, DN and ID which can be seen in Fig. 3A-C. Regression of the EIS responses of the MWCNTs-BSA/GCE on concentrations of DX, DN and ID helped us to obtain the calibration graphs which can be seen as the inset of the Fig. 3A-C. The linear ranges were 0.2–45 μM, 1–100 μM and 0.5–90 μM for DX, DN and ID, respectively. These linear ranges were used to build a calibration set containing DX, DN and ID according to a central composite design.

3.2.2.2. Multivariate calibrations

3.2.2.2.1. Calibration set. Because of the complex matrix of the serum samples we had to apply some strategies which enabled us to use the developed method for the analysis of serum samples. We have used a diluted blank serum sample (drug free) for preparing the samples of the calibration set in it which enabled us to simulate the matrix of the serum sample. According to the linear ranges of the individual calibration curves, a calibration set of 15 samples were prepared which its compositions can be seen in Table 1. The EIS responses of the MWCNTs-BSA/GCE to the mixtures of the calibration set are shown in Fig. 4A.

3.2.2.2.2. Validation set. In order to verify the performance of the developed calibration models by PLS, CPR, RBF-PLS, RBF-ANN and LS-SVM in predicting concentrations of DX, DN and ID, a validation set of 10 samples containing random concentrations of DX, DN and ID based on the linear ranges of their individual calibration graphs was prepared which its composition can be seen in Table 1. The EIS responses of the MWCNTs-BSA/GCE to the samples of the validation set are shown in Fig. 4B. Predicted concentrations of DX, DN and ID in the validation set are presented in Table 2. Performance of the MVC models was compared by evaluating root mean square errors of prediction (RMSEP) and relative error of prediction (REP) according to the

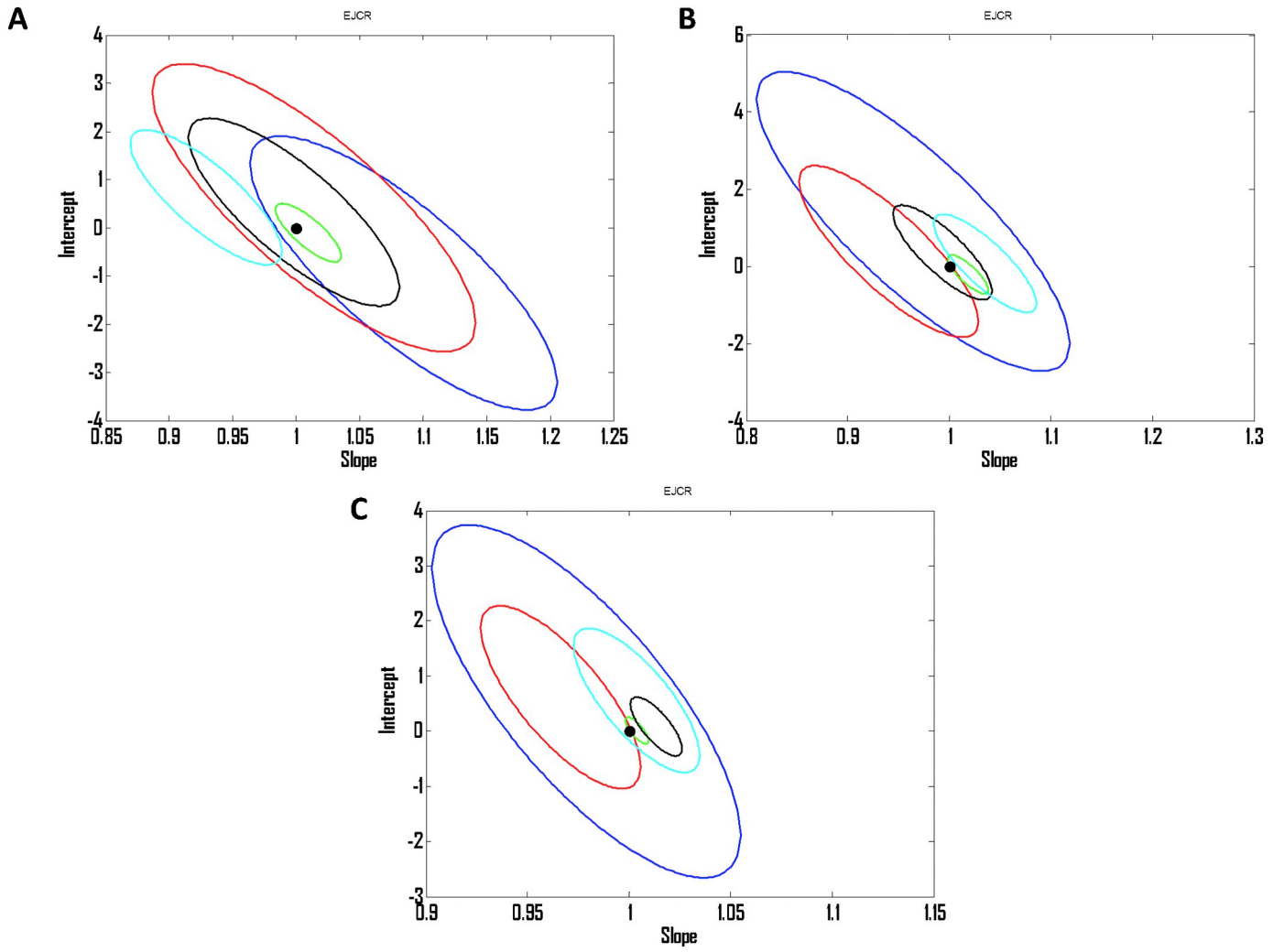

Fig. 6. Ellipses as the outputs of EJCR related to the prediction of (A) DX, (B) DN and (C) ID in validation set. In all cases blue, red, green, black and cyan ellipses are related to PLS, CPR, RBF-PLS, RBF-ANN and LS-SVM, respectively. Black point remarks the ideal point. (For interpretation of the references to colour in this figure legend, the reader is referred to the web version of this article.)

Table 4
Results of the analysis of real samples by RBF-PLS (concentrations are in μM).

Serum 1						
	Spiked			Found (Recovery%)		
DX	45	50	5	45.2 (100.4)	49.5 (101)	4.9 (98)
DN	25	10	40	24.6 (98.4)	10.1 (101)	39.4 (98.5)
ID	35	60	70	35 (100)	61 (101.6)	66 (94.3)
Serum 2						
	Spiked			Found (Recovery%)		
DX	30	75	20	30.3 (101)	76.7 (102.2)	19 (95)
DN	15	80	15	14.6 (97.3)	77 (96.25)	15.2 (101.3)
ID	10	25	40	9.8 (98)	25.3 (101.2)	40 (100)
Serum 3						
	Spiked			Found (Recovery%)		
DX	35	50	30	34 (97.2)	51 (102)	30.5 (101.6)
DN	10	75	60	9.7 (97)	76 (101.3)	57(95)
ID	7	90	20	6.9 (98.6)	88 (97.8)	21 (104.8)

following equations:

$$RMSEP = \sqrt{\frac{\sum_{1}^{n} (y_{pred} - y_{act})^2}{n}} \quad (1)$$

$$REP(\%) = \frac{100}{y_{mean}} \sqrt{\frac{1}{n} \sum_{i=1}^{n} (y_{pred} - y_{act})^2} \quad (2)$$

where y_{act} and y_{pred} are actual and predicted concentrations of each component, respectively, and y_{mean} refer to the mean of the actual concentrations. n is the number of samples in calibration set.

Values of RMSEP and REP are collected in Table 3 which confirms more superiority of the RBF-PLS than the other algorithms. Graphical comparison of the performance of the first-order algorithms based on RMSEP and REP values is shown in Figs. 5A and B, respectively. As can be seen, RBF-PLS has more superiority than the other algorithms. In order to further comparison of the performance of the developed MVC models, elliptical joint confidence region (EJCR) was used [25,26] which performs an ordinary least squares (OLS) analysis of predicted concentrations on nominal ones [25]. The EJCR compares calculated intercept and slope with their theoretically values (intercept = 0, slope = 1), if the ellipses contains the ideal point, the predicted and nominal concentrations are not different at the level of 95% confidence and the elliptic size reflects precision of the analytical method, smaller size corresponds to higher precision [26]. The results of EJCR are shown in Fig. 6. As can be seen, the ellipse of RBF-PLS (green ellipse) is smaller than those of the other algorithms which confirms more precision of the RBF-PLS than the other algorithms. For DN and ID, the ideal point falls onto the ellipse of RBF-PLS which confirms that the

RBF-PLS has more accuracy in predicting concentration of DX than DN and ID. We chose RBF-PLS for the analysis of real samples towards simultaneous determination of DX, DN and ID.

3.3. Performance assessment of the developed methodology in the analysis of real samples

In order to evaluate performance of the RBF-PLS for prediction of concentration of DX, DN and ID in real samples, three blank human serum samples described in Section 2.4 were chosen as real cases. 5 mL from each serum samples were diluted with 5 mL PBS (0.1 M, pH 7.4) and then, were spiked with different concentrations of DX, DN and ID as are presented in Table 4. Then, concentrations of the spiked samples were predicted with help of RBF-PLS and the results are presented in Table 4. The recoveries showed that the RBF-PLS was successful in prediction of concentrations of DX, DN and ID in real samples.

4. Conclusions

In this work, we have developed a novel impedimetric approach assisted by first-order multivariate calibration for simultaneous determination of DX, DN and ID in serum samples for the first time. First-order impedimetric data in coupling with several first-order MVC algorithms such as PLS, CPR, RBF-PLS, RBF-ANN and LS-SVM showed different predictive abilities and among them the RBF-PLS had the best performance for prediction of concentrations of DX, DN and ID. After checking performance of the mentioned algorithms in simultaneous prediction of concentrations of DX, DN and ID by statistical and graphical methods, the RBF-PLS was chosen as the best one for the analysis of real samples. Fortunately, application of the RBF-PLS to the spiked serum samples towards simultaneous determination of DX, DN and ID was acceptable. Good recoveries guaranteed its successfulness in the analysis of real samples. Sensitivity of developed analytical method in this work was benefited from impedimetry and modification of the bare GCE while selectivity of the method was improved by exploiting first-order advantage from impedimetric data. On the whole, by the combination of first-order impedimetric data and first-order multivariate calibration we have developed a novel electroanalytical method for simultaneous determination of DX, DN and ID in real samples.

Statement

All the authors contributed equally in all sections of the project.

Declaration of Competing Interest

The authors declare that they have no known competing financial interests or personal relationships that could have appeared to influence the work reported in this paper.

Acknowledgements

The financial supports of this project by research council of Kermanshah University of Medical Sciences are gratefully acknowledged.

References

[1] GBD, Disease and injury incidence and prevalence, collaborators. “global, regional, and national incidence, prevalence, and years lived with disability for 310 diseases and injuries, 1990-2015: a systematic analysis for the global burden of disease study 2015”, Lancet 388 (2016) (2015) 1545–1602.
[2] O. Wolach, R.M. Stone, How I treat mixed-phenotype acute leukemia, Blood 125 (2015) 2477–2485.
[3] A.L. Demain, P. Vaishnav, Natural products for cancer chemotherapy, Microb. Biotechnol. 4 (2011) 687–699.
[4] A. Zangeneh, M.M. Zangeneh, Green synthesis and chemical characterization of gold nanoparticle synthesized using *Camellia sinensis* leaf aqueous extract for the treatment of acute myeloid leukemia in comparison to daunorubicin in a leukemic mouse model, Appl. Organomet. Chem. (2019) e5290.
[5] M.M. Zangeneh, A. Zangeneh, Novel green synthesis of *Hibiscus sabdariffa* flower extract conjugated gold nanoparticles with excellent anti-acute myeloid leukemia effect in comparison to daunorubicin in a leukemic rodent model, Appl. Organomet. Chem. (2019) e5271.
[6] S. Hemmati, Z. Joshani, A. Zangeneh, M.M. Zangeneh, Green synthesis and chemical characterization of *Thymus vulgaris* leaf aqueous extract conjugated gold nanoparticles for the treatment of acute myeloid leukemia in comparison to doxorubicin in a leukemic mouse model, Appl. Organomet. Chem. (2019) e5267.
[7] N. Bahner, P. Reich, D. Frense, M. Menger, K. Schieke, D. Beckmann Anal, Bioanal. An aptamer-based biosensor for detection of doxorubicin by electrochemical impedance spectroscopy, Anal. Bioanal. Chem. 410 (2018) 1453–1462.
[8] S.N. Mahnik, K. Lenz, N. Weissenbacher, R.M. Mader, M. Fuerhacker, Fate of 5-fluorouracil, doxorubicin, epirubicin, and daunorubicin in hospital wastewater and their elimination by activated sludge and treatment in a membrane-bio-reactor system, Chemosphere 66 (2007) 30–37.
[9] J.S. Mandeville, E. Froehlich, H.A. Tajmir-Riahi, Study of curcumin and genistein interactions with human serum albumin, J. Pharm. Biomed. Anal. 49 (2009) 468–474.
[10] H.X. Luo, Y. Du, Z.X. Guo, Electrochemistry of N-n-undecyl-N′-(sodium-pamino-benzenesulfonate) thiourea and its interaction with bovine serum albumin, Bioelectrochemistry 74 (2009) 232–235.
[11] C. Bertucci, V. Andrisano, R. Gotti, V. Cavrini, Use of an immobilised human serum albumin HPLC column as a probe of drug–protein interactions: the reversible binding of valproate, J. Chromatogr. B 768 (2002) 147–155.
[12] Q.H. Lu, C.D. Ba, D.Y. Chen, Investigating noncovalent interactions of rutin – serum albumin by capillary electrophoresis – frontal analysis, J. Pharm. Biomed. Anal. 47 (2008) 888–891.
[13] B. Bojko, A. Sulkowska, M. Maciazek-Jurczyk, J. Rownicka, W.W. Sulkowski, Investigations of acetaminophen binding to bovine serum albumin in the presence of fatty acid: fluorescence and 1H NMR studies, J. Mol. Struct. 924-926 (2009) 332–337.
[14] G. Mohammadi, E. Faramarzi, M. Mahmoudi, S. Ghobadi, A.R. Ghiasvand, H.C. Goicoechea, A.R. Jalalvand, Chemometrics-assisted investigation of interactions of Tasmar with human serum albumin at a glassy carbon disk: application to electrochemical biosensing of electro-inactive serum albumin, J. Pharm. Biomed. Anal. 156 (2018) 23–35.
[15] M.B. Gholivand, A.R. Jalalvand, H.C. Goicoechea, R. Gargallo, Th. Skov, Chemometrics: an important tool for monitoring interactions of vitamin B7 with bovine serum albumin with the aim of developing an efficient biosensing system for the analysis of protein, Talanta 132 (2015) 354–365.
[16] R. Khodarahmi, Sh. Khateri, H. Adibi, V. Nasirian, M. Hedayati, E. Faramarzi, Sh. Soleimani, H.C. Goicoechea, A.R. Jalalvand, Chemometrical-electrochemical investigation for comparing inhibitory effects of quercetin and its sulfonamide derivative on human carbonic anhydrase II: theoretical and experimental evidence, Int. J. Biol. Macromol. 136 (2019) 377–385.
[17] M.B. Gholivand, A.R. Jalalvand, H.C. Goicoechea, R. Gargallo, T. Skov, G. Paimard, Combination of electrochemistry with chemometrics to introduce an efficient analytical method for simultaneous quantification of five opium alkaloids in complex matrices, Talanta 131 (2015) 26–37.
[18] M.B. Gholivand, A.R. Jalalvand, H.C. Goicoechea, Multivariate analysis for resolving interactions of carbidopa with dsDNA at a fullerene-C_{60}/GCE, Int. J. Biol. Macromol. 69 (2014) 369–381.
[19] A.R. Jalalvand, H.C. Goicoechea, D.N. Rutledge, Applications and challenges of multi-way calibration in electrochemical analysis, Trends Anal. Chem. 87 (2017) 32–48.
[20] A.R. Jalalvand, H.C. Goicoechea, Applications of electrochemical data analysis by multivariate curve resolution-alternating least squares, Trends Anal. Chem. 88C (2017) 134–166.
[21] K. Ghanbari, M. Roushani, F. Farzadfar, H.C. Goicoechea, A.R. Jalalvand, Developing a four-dimensional voltammetry as a powerful electroanalytical methodology for simultaneous determination of three colorants in the presence of an uncalibrated interference, Chemom. Intell. Lab. Syst. 189 (2019) 27–38.19.
[22] M.B. Gholivand, A.R. Jalalvand, H.C. Goicoechea, T. Skov, Fabrication of an ultrasensitive impedimetric buprenorphine hydrochloride biosensor from computational and experimental angles, Talanta 124 (2014) 27–35.
[23] M.B. Gholivand, A.R. Jalalvand, H.C. Goicoechea, Developing a novel computationally designed impedimetric pregabalin biosensor, Electrochim. Acta 133 (2014) 123–131.
[24] J.H. Suh, Y.Y. Lee, H.J. Lee, M. Kang, Y. Hur, S.N. Lee, D.H. Yang, S.B. Han, J. Pharm. Biomed. Anal. 75 (2013) 214–219.
[25] A.G. Gonzalez, M.A. Herrador, A.G. Asuero, Intra-laboratory testing of method accuracy from recovery assays, Talanta 48 (1999) 729–736.
[26] J.A. Arancibia, G.M. Escandar, Two different strategies for the fluorimetric determination of piroxicam in serum, Talanta 60 (2003) 1113–1121.